

ARTICLE

Large Scale Homogeneous Growth Mechanics of Microcrystalline Silicon Films on Rough Surface

Wen-feng Zhao^{a,b}, Jun-fang Chen^{a*}, Yan Wang^a, Ran Meng^a, Yi-ran Zhao^a, Shi-yun Shao^a, Ji-yun Li^b, Yun Zhang^b

a. School of Physics and Telecommunication Engineering, Laboratory of Quantum Information Technology, South China Normal University, Guangzhou 510006, China

b. College of Engineering, South China Agricultural University, Guangzhou 510642, China

(Dated: Received on January 7, 2010; Accepted on June 23, 2010)

Large scale homogenous growth of microcrystalline silicon ($\mu\text{c-Si:H}$) on cheap substrates by inductively coupled plasma (ICP) of Ar diluted SiH_4 has been studied. From XRD and Raman spectrum, we find that substrates can greatly affect the crystalline orientation, and the $\mu\text{c-Si:H}$ films are comprised of small particles. Thickness detection by surface profilometry shows that the thin $\mu\text{c-Si:H}$ films are homogenous in large scale. Distributions of both ion density and electron temperature are found to be uniform in the vicinity of substrate by means of diagnosis of Langmuir probe. Based on these experimental results, it can be proposed that rough surfaces play important roles in the crystalline network formation and Ar can affect the reaction process and improve the characteristics of $\mu\text{c-Si:H}$ films. Also, ICP reactor can deposit the thin film in large scale.

Key words: Microcrystalline silicon film, Inductively coupled plasma, Rough surface

I. INTRODUCTION

Microcrystalline silicon ($\mu\text{c-Si:H}$) thin film has been intensively studied as the material used in photovoltaic (PV) solar cells with high conversion efficiency and high stability because of the well mastered technology even at low deposition temperature and the possibility to deposit $\mu\text{c-Si:H}$ thin films on different substrates [1]. In the last couple years, many authors have already researched the $\mu\text{c-Si:H}$ characteristics and obtained different kinds of applications [2]. For the existing industrial processes, crucial parameters for low-cost production of thin-film solar cell are the low cost substrate and its scale as large as possible, which would still preserve the materials quality [3].

A stainless steel is widely used as substrate because of its cheap and flexible characteristics [4]. Roll-to-roll manufacture of amorphous silicon has been applied to thin film solar cell [5]. The amorphous thin film solar cell based on stainless steel substrate has been deposited at low temperature [6].

Inductively coupled plasma (ICP) is one of the promising plasma sources and has powerful applications in the semiconductor industry and film deposition. It has been reported that ICP has such advantages as high ion density (10^{10} – 10^{12} cm^{-3}), a decline in ion dam-

age, and independently controllable ion energy. In addition, ICP need not to require external magnetic fields. This makes ICP sources most attractive [7]. Park *et al.* built an array of inductively coupled plasma sources for large area plasma [8].

In this work, we use Ar-diluted SiH_4 as feedstock gas to deposit large scale thin $\mu\text{c-Si:H}$ films in ICP reactor on c-Si, stainless steel and glass substrates at 150 °C. These studies highlight the important role of the substrate surfaces in the nucleation of silicon crystallites. And we discuss the mechanism of depositing $\mu\text{c-Si:H}$ films in large scale.

The characteristic Ar plasma in the vicinity of substrate in large scale is studied. Distributions of both ion density and electron temperature are uniform.

II. EXPERIMENTS

The $\mu\text{c-Si:H}$ thin films were deposited at 6 cm \times 2 cm c-Si, 6 cm \times 2 cm stainless steel and 6 cm \times 2 cm Corning 7101 glass substrates with ICPECVD at 150 °C [9]. The stainless steel wafer was slapped in order to increase the surface roughness. The thin films were grown by ICPECVD at frequency 13.56 MHz. Several samples were deposited under the conditions that argon dilution in the gas mixture $R(\text{SiH}_4/(\text{SiH}_4+\text{Ar}))=5\%$, while the radius of substrate holder size was 6 cm, the chamber pressure was 0.5 Pa, and the power was 120 W, respectively.

The deposited films were structurally character-

* Author to whom correspondence should be addressed. E-mail: chenjf@sclu.edu.cn, Tel.: +86-20-85214371

ized by the LabRAM Aramis Raman spectroscopy of HORIBA Jobin Yvon. Raman scattering spectra were measured under a right-angle of scattering geometry, in which a 532.8 nm light was incident to the film surface in an Ar gas atmosphere. The X'Pert Pro MPD X-ray diffractometer (XRD) of PANalytical was applied for estimating the crystallinity. Thickness of samples was investigated by Xp-1 surface profilometry of the Ambios Technology, Inc.

A single Langmuir probe was inserted in the chamber. By revolving the probe head and calculating the angle, both ion density and electron temperature in the vicinity of substrate were obtained.

By recording the current through Langmuir probe as a function of the applied voltage, the I - V characteristic was obtained and the data were used to calculate electron temperature and ion density. All calculations of plasma parameters were performed through a PC by using suitable software. The electron temperature $k_B T_e$, is determined in electron volts by the equation:

$$k_B T_e = \left(\Delta \frac{I_e}{\Delta V} \right)^{-1} \quad (1)$$

The ion density (n_i) was obtained from the electron saturation current by the equation

$$I_e = A e n_i \sqrt{\frac{k_B T_e}{2\pi m}} \quad (2)$$

where A is the probe area, e is the magnitude of the electronic charge, m is the electronic mass and k_B is the Boltzmann constant [10].

III. RESULTS AND DISCUSSION

In Ar plasma, the measured ion density distribution and electron temperature in the vicinity of substrate are shown in Fig.1 under the RF power of 120 W and discharge pressure of 0.5 Pa. Figure 1 shows that the radial distributions of both ion density and electron temperature are essentially uniform. The measured ion density and electron temperature change slightly from $0.25 \times 10^{10} \text{ cm}^{-3}$ to $0.3 \times 10^{10} \text{ cm}^{-3}$ and from 2.9 eV to 3.7 eV, respectively. It is useful for device processing and materials preparation with specific need to reduce ion impact damage. Due to the influence of gas flow, both ion density and electron temperature near the outlet are effectively changed [11].

In order to obtain a better understanding of deposition mechanism of $\mu\text{-Si:H}$ films in the large scale and its relation to the deposition process, the film thickness was measured by surface profilometry. As shown in Fig.2 the thickness of each sample decreases with radial position. The change of thin film thickness is 10% on the c-Si substrate, about 20% on the stainless steel substrate, and approximately 30% on the glass substrate. We know one reason affecting thin films deposition rate

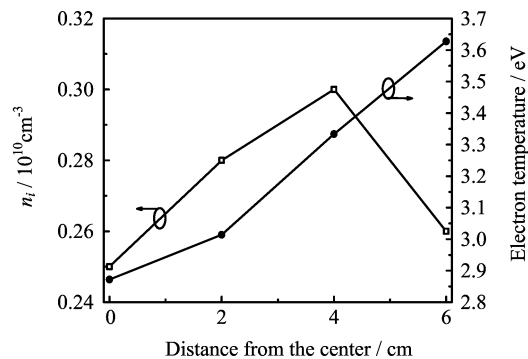


FIG. 1 Distribution of ion density and electron temperature in the vicinity of substrate in ICP reactor.

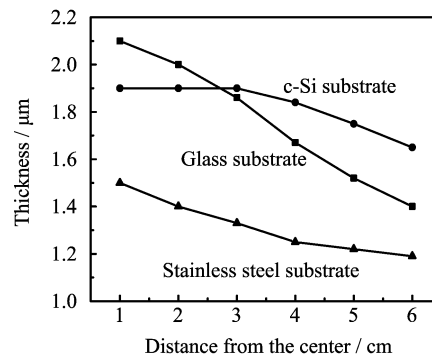


FIG. 2 The thickness of samples with different distance from the center.

is sticking coefficient and evaporation coefficient [12]. The c-Si substrate has large sticking coefficient for the $\mu\text{-Si:H}$ films and the stainless steel substrate has rough surface to increase the sticking effect. The glass substrate has small sticking coefficient and is easily affected by gas flow which makes the nucleate float easily. And during the deposition process, the non-uniformity of gas flow leads to the different evaporation rate on the surface of the glass substrate. It could be the reason that the thin film on the glass substrate has large thickness gradient. So the $\mu\text{-Si:H}$ films on the c-Si and stainless steel substrates are homogeneous in a large scale.

The thin films are studied by XRD analysis. Figure 3 shows the thin films have an amorphous character on the glass substrate and have an orientation along the (111) on the c-Si substrate. On the stainless steel substrate, three orientations are observed. From Fig.3, FWHM of the thin film on the stainless steel substrate is smaller than that on the c-Si substrate. The FWHM is inversely proportional to crystalline size, which proves that particles on the stainless substrate are larger.

Through slapping the stainless steel substrate, the surface roughness can be greatly increased. Due to large local slopes of surface topology appeared, re-emission is believed to occur. So the ions can impact surface many times during the deposition procedure.

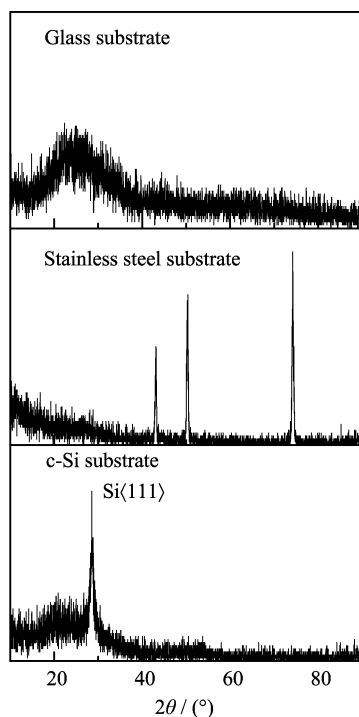


FIG. 3 The XRD pattern of $\mu\text{c-Si:H}$ thin films on different substrates.

The collisions into the bond-centered location facilitate rearrangement of the amorphous Si network to crystallize and the growth of nanocrystalline silicon even at very low temperatures. In the disorder-to-order transformation, the collisions of atoms or ions with Si–Si bonds provide new pathways in which Si atoms can rearrange. Specifically, bond breaking and reforming reactions are facilitated by collision, which results in elimination of strained Si–Si bonds and concerted atomic rearrangements. These atomic-scale mechanisms play an important role in the nucleation and growth of the nanocrystalline Si structure [13]. Then crystalline nucleation takes place on the rough surface of stainless steel substrate. Due to random collision, the crystalline particles have three orientations in the XRD pattern.

Figures 4 and 5 show Raman spectra acquired two typical $\mu\text{c-Si}$ films. Considering fitted Gaussian peaks which can be ascribed to different phases, an analysis of the Raman spectra in the region $350\text{--}550\text{ cm}^{-1}$ has been performed. The narrow feature centred at $518\text{--}521\text{ cm}^{-1}$ is due to a crystalline phase; the broad peak at $508\text{--}513\text{ cm}^{-1}$ is ascribable to small crystallites or grain boundaries; the broad peak at $480\text{--}495\text{ cm}^{-1}$ has been assigned to the amorphous-like phase [14].

From the fitted Gaussian peak, the thin films on both the c-Si and the stainless steel substrates are comprised of amorphous phase and small crystallites. As usual, it is difficult to deposit the $\mu\text{c-Si:H}$ thin film on the stainless steel substrate. Through increasing the sur-

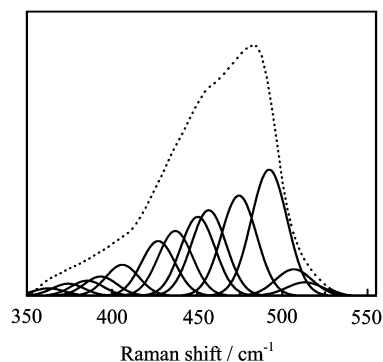


FIG. 4 Raman spectra of $\mu\text{c-Si:H}$ thin films on stainless steel substrate (dotted line) and fitted Gaussian function (solid lines). Crystalline fraction is 26%.

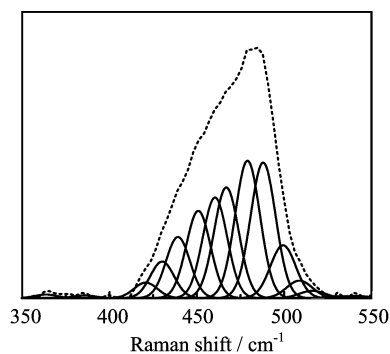


FIG. 5 Raman spectra of $\mu\text{c-Si:H}$ thin films on c-Si substrate (dotted line) and fitted Gaussian function (solid lines). Crystalline fraction is 22%.

face roughness of stainless steel, we obtain the same crystalline fraction as that on the c-Si substrate.

The crystalline fraction of $\mu\text{c-Si:H}$ films that maintain the suitable value is beneficial to high efficient solar cell. Small grains and intermediate range order may play important roles in improving the stability [15]. The crystalline fraction is small in order to keep the absorption coefficient close to the amorphous material, while the improvement of the short range order leads to better electronic performance of the materials [16]. In our experiment, due to columnar growth of the $\mu\text{c-Si:H}$ film along the direction perpendicular to the rough surface of stainless steel, the microcrystalline phase distribution of $\mu\text{c-Si:H}$ films is mainly dependent on the surface topography and crystalline fraction of the thin films maintains suitable value [17].

Through using SiH_4 and Ar gas as feedstock gas, crystalline volume fraction are greater for argon plasma etching than hydrogen. The reason is argon atoms and ions have higher energy than hydrogen atoms and can break Si–Si bonds easily. Etching model has been proposed based on the experimental fact. Si–Si bonds which preferentially weak bonds involving in the amorphous network structure are broken after atomic H

reaches the film-growing surface. This leads to a removal of Si atoms weakly bonded to another Si. This site is replaced with a new film precursor SiH₃ which creates strong and rigid Si–Si bond and gives rise to an ordered structure [18]. By use of argon rather than hydrogen etching, the combination of higher energy and larger mass can give a higher energy to the film and also cause the larger growth of crystalline grains [19].

ICP reactor can generate the homogeneous ion density and electron temperature in the vicinity of substrate which is beneficial to deposit the uniform $\mu\text{c-Si:H}$ films in large scale. What's more, we can control the gas flow velocity distribution to make $\mu\text{c-Si:H}$ films homogeneous in large scale. Similarly, the rough surface can increase the uniformity of $\mu\text{c-Si:H}$ films in large scale [20].

IV. CONCLUSION

It is evident that low cost is trend for $\mu\text{c-Si:H}$ films deposition. Using Ar-diluted SiH₄ gas as feedstock gas, we have succeeded in obtaining $\mu\text{c-Si:H}$ films in ICP reactor at c-Si and stainless steel substrates.

From analysis by XRD and Raman, we have found that the substrate can greatly affect the crystalline orientation and the $\mu\text{c-Si:H}$ films are comprised of small particles in our experiments. The $\mu\text{c-Si:H}$ films deposited on stainless steel substrate have several orientations by increasing the surface roughness. The rough surface plays an important role in the crystalline network formation. Then roll to roll technology based on cheap stainless steel substrate has a new method for preparing the $\mu\text{c-Si:H}$ films. Also, Ar can affect the reaction process and improve the $\mu\text{c-Si:H}$ films characteristics.

Thickness detected by surface profilometry shows that the thin $\mu\text{c-Si:H}$ films are homogenous in large scale. Distributions of both the ion density and the electron temperature are homogeneous in the vicinity of substrate. It can be proposed that inductively coupled plasma reactor can deposit the thin film in large scale.

V. ACKNOWLEDGMENTS

This work was supported by the National Natural Science Foundation of China (No.10575039) and the Chi-

nese Specialized Research Fund for the Doctoral Program of Higher Education (No.2004057408).

- [1] N. Phama, Y. Djeridane, A. Abramov, A. Hadjadj, and P. Roca i Cabarrocas, *Mater. Sci. Eng. B* **159-160**, 27 (2009).
- [2] N. Pham, A. Hadjadj, P. Roca i Cabarrocas, O. Jbara, and F. Kail, *Thin Solid Films* **517**, 6225 (2009).
- [3] A. G. Aberle, *Thin Solid Films* **517**, 4706 (2009).
- [4] H. Li, R. L. Stolk, C. H. M. van der Werf, M. Y. S. Rusche, J. K. Rath, and R. E. I. Schropp, *Thin Solid Films* **501**, 276 (2006).
- [5] M. Izu and T. Ellison, *Sol. Energy Mater. Sol. Cells* **78**, 613 (2003).
- [6] M. Brinza, J. K. Rath, and R. E. I. Schropp, *Sol. Energy Mater. Sol. Cells* **93**, 680 (2009).
- [7] M. H. Lee, S. H. Jang, and C. W. Chung, *Phys. Plasmas* **13**, 053502 (2006).
- [8] S. G. Park, C. Kim, and B. H. O, *Thin Solid Films* **355**, 252 (1999).
- [9] W. F. Zhao, J. F. Chen, and R. Meng, *Spectrosc. Spectr. Anal.* **29**, 3134 (2009).
- [10] A. Qayyum, M. Ikram, M. Zakaullah, A. Waheed, G. Murtza, R. Ahmad, A. Majeed, N. A. D. Khattak, K. Mansoor, and K. A. Chaudhary, *Int. J. Mod. Phys. B* **17**, 2749 (2003).
- [11] P. Buchner, H. Ferfers, H. Schubert, and J. Uhlenbusch, *Plasma Sources Sci. Technol.* **6**, 450 (1997).
- [12] W. H. Lin, Z. L. Liu, and K. L. Yao, *Acta Phys. Sin.* **49**, 791 (2000).
- [13] S. Sriraman, S. Agarwal, E. S. Aydil, and D. Maroudas, *Nature* **418**, 62 (2002).
- [14] M. M. Giangregorio, M. Losurdo, A. Sacchetti, P. Capezzuto, F. Giorgis, and G. Bruno, *Appl. Surf. Sci.* **253**, 287 (2006).
- [15] G. Z. Yue, B. J. Yan, G. Ganguly, J. Yang, and S. Guha, *Appl. Phys. Lett.* **88**, 263507 (2006).
- [16] L. Raniero, I. Ferreira, L. Pereira, H. Águas, E. Fortunato, and R. Martins, *J. Non-Cryst. Solids* **352**, 1945 (2006).
- [17] E. Vallat-Sauvain, J. Bailat, J. Meier, X. Niquile, U. Kroll, and A. Shah, *Thin Solid Films* **485**, 77 (2005).
- [18] A. Matsuda, *J. Non-Cryst. Solids* **338-340**, 1 (2004).
- [19] J. H. Yoon, *J. Non-Cryst. Solids* **353**, 4223 (2007).
- [20] Y. J. Yan, G. F. Hou, J. M. Xue, X. Y. Han, Y. Z. Liu, X. Y. Yang, L. J. Liu, P. Dong, Y. Zhao, and X. H. Geng, *Acta Phys. Sin.* **57**, 3892 (2008).